

Incommensurate magnetic order and dynamics induced by spinless impurities in $\text{YBa}_2\text{Cu}_3\text{O}_{6.6}$

A. Suchaneck,¹ V. Hinkov,¹ D. Haug,¹ L. Schulz,² C. Bernhard,²
A. Ivanov,³ K. Hradil,⁴ C.T. Lin,¹ P. Bourges,⁵ B. Keimer,^{1,*} and Y. Sidis^{5,†}

¹Max Planck Institute for Solid State Research, D-70569 Stuttgart, Germany

²Physics Department and Fribourg Center for Nanomaterials, Fribourg University, CH-1700 Fribourg, Switzerland

³Institut Laue-Langevin, 156X, F-38042 Grenoble Cedex 9, France

⁴Institute for Physical Chemistry, University of Göttingen, D-37077 Göttingen, Germany

⁵Laboratoire Léon Brillouin, CEA-CNRS, CE-Saclay, F-91191 Gif-sûr-Yvette, France

We report an inelastic-neutron-scattering and muon-spin-relaxation study of the effect of 2% spinless (Zn) impurities on the magnetic order and dynamics of $\text{YBa}_2\text{Cu}_3\text{O}_{6.6}$, an underdoped high-temperature superconductor that exhibits a prominent spin-pseudogap in its normal state. Zn substitution induces static magnetic order at low temperatures and triggers a large-scale spectral-weight redistribution from the magnetic resonant mode at 38 meV into uniaxial, incommensurate spin excitations with energies well below the spin-pseudogap. These observations indicate a competition between incommensurate magnetic order and superconductivity close to a quantum critical point. Comparison to prior data on $\text{La}_{2-x}\text{Sr}_x\text{CuO}_4$ suggests that this behavior is universal for the layered copper oxides and analogous to impurity-induced magnetic order in one-dimensional quantum magnets.

PACS numbers: 75.10.Kt, 74.72.Kf, 74.72.Gh, 74.25.Dw

Spinless impurities have provided key insights into the spin correlations of low-dimensional quantum magnets. Research on quasi-one-dimensional (1D) quantum-disordered magnets with a spin gap has shown that every magnetic vacancy contributes to a Curie term in the uniform susceptibility and generates a cloud of antiferromagnetically correlated spins whose spatial extent is inversely proportional to the gap [1]. The striking discovery that a dilute concentration of spinless impurities induces antiferromagnetic long-range order in a spin-Peierls system [2] can be attributed to constructive interference between spin-polarization clouds centered at different impurities. Related “order from disorder” phenomena were later observed in a wide class of quasi-1D systems and shown to exhibit universal characteristics [3, 4]. In contrast to the comprehensive understanding that has been developed for 1D magnets, theoretical work on spinless impurities in 2D quantum magnets has thus far been restricted to analytical calculations at quantum critical points [5–8] and numerical simulations for specific 2D spin Hamiltonians with quantum-disordered ground states [9]. Both approaches predict impurity-induced spin textures and order-from-disorder phenomena not unlike those observed in 1D magnets. Experimental tests of these predictions have, however, proven difficult because of the paucity of physical realizations of 2D spin liquids and the limited chemical solubility of nonmagnetic atoms in specific compounds.

Layered copper oxides have been a fruitful testing ground for theories of 2D quantum magnetism and for the behavior of spinless impurities in two dimensions, despite additional complications introduced by the presence of itinerant charge carriers and *d*-wave superconductivity [1, 10]. Spinless impurities can be readily introduced into the CuO_2 planes by replacing spin-1/2 copper ions by nonmagnetic zinc or lithium. A large body of nuclear magnetic resonance (NMR) experiments on metallic and superconducting $\text{YBa}_2\text{Cu}_3\text{O}_{6+x}$

(YBCO_{6+x}) has demonstrated that such impurities generate a Curie term in the uniform susceptibility and a staggered spin polarization cloud on neighboring Cu sites, in close analogy to the 1D systems discussed above [1]. NMR experiments on other families of cuprates are much more limited, because intrinsic disorder due to dopant atoms broadens the NMR lines, so that the effect of Zn impurities is masked by native disorder [11]. Inelastic neutron scattering (INS) experiments on both YBCO_{6+x} and $\text{La}_{2-x}\text{Sr}_x\text{CuO}_4$ (LSCO) have revealed Zn-induced low-energy spin excitations, in qualitative agreement with the NMR results. In contrast to the 1D systems [4], however, a universal picture of the impurity-induced magnetism has not yet emerged in the 2D cuprates, because the spatial character of the impurity-induced low-energy spin dynamics in both materials appeared to be rather different: commensurate antiferromagnetic in YBCO_{6+x} [12, 13] and incommensurate (IC) in LSCO [14, 15]. Moreover, Zn-induced static incommensurate magnetism, which was observed in LSCO [14–16] and interpreted as evidence of pinning of fluctuating stripes [17], has thus far not been detected in YBCO_{6+x} . For this reason, and because LSCO exhibits static IC magnetic order at some doping levels even in the absence of spinless impurities [18, 19], the universality of this “order from disorder” phenomenon has been questionable. These considerations have motivated us to revisit the effect of spinless impurities on the magnetic correlations of $\text{YBCO}_{6.6}$, a material with minimal native disorder that is well known for its large normal-state spin-pseudogap [1].

The experiments were performed on an array of detwinned, co-aligned $\text{YBa}_2(\text{Cu}_{0.98}\text{Zn}_{0.02})_3\text{O}_{6.6}$ (henceforth $\text{YBCO}_{6.6}\text{:Zn}$) single crystals of total mass 650 mg and superconducting $T_c = 30$ K. The Zn content was determined by energy-dispersive x-ray analysis and inductively-coupled plasma spectroscopy. A twin domain population ratio of

4:1 enabled us to discriminate spin excitations propagating along the a - and b -axes in the CuO_2 planes, which is important in view of the recent observation of uniaxial, incommensurate magnetism in $\text{YBCO}_{6.45}$ [20, 21]. The INS measurements were carried out on the spectrometers IN8 (Institut Laue-Langevin, Grenoble), 4F2, 1T, 2T (Orphée, Laboratoire Léon Brillouin, Saclay), and PUMA (FRM-II, Garching), using either a pyrolytic-graphite (PG) (002) or a Si (111) monochromator in combination with a PG (002) analyzer. PG filters extinguished higher-order contaminations of the beam. The final wave vector was fixed to 4.1 \AA^{-1} for excitation energies $E \geq 25 \text{ meV}$, and to 2.662 \AA^{-1} or 1.97 \AA^{-1} for $E < 25 \text{ meV}$. Reference measurements were performed on a Zn-free $\text{YBCO}_{6.6}$ array with $T_c = 61 \text{ K}$ described previously [22]. Data on both arrays were compared by calibration measurements on the optical phonon at 42.5 meV following previous work [23], and by performing measurements under identical conditions. The wave vector transfers $\mathbf{Q} = (H, K, L)$ are given in units of the reciprocal-lattice vectors \mathbf{a}^* , \mathbf{b}^* , and \mathbf{c}^* . $Q = (H, K)$ stands for 2D projections of \mathbf{Q} , and $Q_{AF} = (0.5, 0.5)$ is the wave vector characterizing antiferromagnetism in undoped $\text{YBCO}_{6.0}$.

Figure 1a,b shows INS scans taken along the a -axis of $\text{YBCO}_{6.6}\text{:Zn}$ at $E = 5 \text{ meV}$, well below the spin pseudogap of pristine $\text{YBCO}_{6.6}$. A pair of well separated IC peaks symmetrically displaced from Q_{AF} is observed consistently in two Brillouin zones on top of an extraneous background arising from the sample mount. The background is independent of the sample orientation and can be readily subtracted (Fig. 1c). The signal is absent at $L = 0$ and vanishingly small at large $|\mathbf{Q}|$, and can thus be ascribed to acoustic spin fluctuations [23]. Very similar peaks are also observed at $E = 7$ and 10 meV (Fig. 1d,e). As scans along the b -axis are peaked at Q_{AF} , the excitations are characteristic of uniaxial IC magnetism. Since low-energy spin excitations of comparable intensity are not observed in control experiments on pristine $\text{YBCO}_{6.6}$ (see below), they can be identified as a result of Zn substitution.

The incommensurability of the impurity-induced spin excitations eluded detection in previous INS experiments on $\text{YBCO}_{6+x}\text{:Zn}$ [12, 13] for three reasons: First, the signal from the previously investigated twinned crystals consists of equal contributions from two twin domains, so that the IC character is less apparent. Second, earlier studies were performed in the scattering plane spanned by the vectors $\mathbf{Q} = (1, 1, 0)$ and $(0, 0, 1)$, which does not include the IC wave vector. Third, the effective momentum-space resolution in the latter configuration is poorer than in the present experiment, because the long, vertical axis of the resolution ellipsoid is parallel to the CuO_2 -planes.

The INS profiles were fitted to Gaussians centered at $Q_{AF} \pm (\delta, 0)$ (lines in Figs. 1c-e). In the range $E = 5 - 10 \text{ meV}$, both the incommensurability $\delta = 0.10 \pm 0.05$ and the intrinsic half-width-at-half-maximum $\Delta Q = 0.055 \pm 0.025$ extracted from these fits were found to be energy independent within the error. The incommensurability is consistent

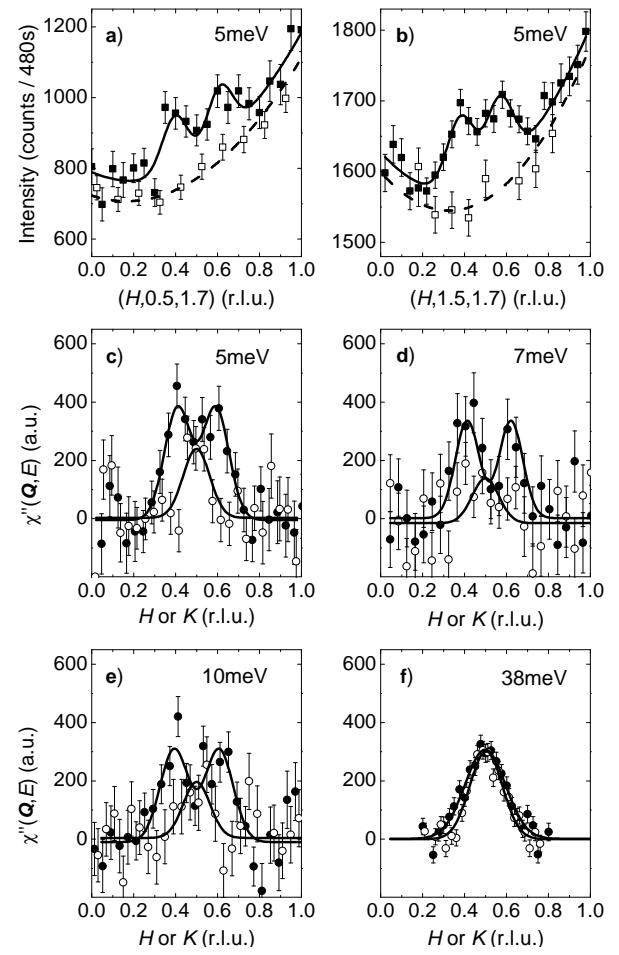


FIG. 1: Constant-energy scans in $\text{YBCO}_{6.6}\text{:Zn}$ at $T = 10 \text{ K}$. (a,b) Uncorrected scans along (a) $\mathbf{Q} = (H, 0.5, 1.7)$ and (b) $(H, 1.5, 1.7)$. The extraneous background was determined by rotating the sample by a) 30° , b) 10° and repeating the scans (open symbols). (c-f) Background-corrected scans along $\mathbf{Q} = (H, 1.5, 1.7)$ (full symbols) and $(1.5, K, 1.7)$ (open symbols) at $E = 5, 7, 10$, and 38 meV .

with the one that characterizes excitations above the spin-pseudogap of pristine $\text{YBCO}_{6.6}$ [22], but significantly larger than the one observed in $\text{YBCO}_{6.45}$ [20]. This confirms that the Zn content and the doping level are independent control parameters [1]. Models according to which Zn impurities reduce the hole doping level [24, 25] are inconsistent with our data. The intrinsic momentum width translates into a length scale of $\xi = 2.9a$, where a is the in-plane lattice spacing. This represents a lower bound on the intrinsic coherence length of the spin fluctuations, because inhomogeneous broadening (arising from the doping dependence of δ in combination with a possible slight nonuniformity of the doping level) may also contribute to ΔQ . In any case, the value of ξ determined in this way is in good agreement with NMR data [26] and comparable to $5.8a$, the mean distance between Zn impurities in the CuO_2 planes.

In view of the sharp excitation peaks, we have investigated the presence of magnetic order in $\text{YBCO}_{6.6}\text{:Zn}$. Since a

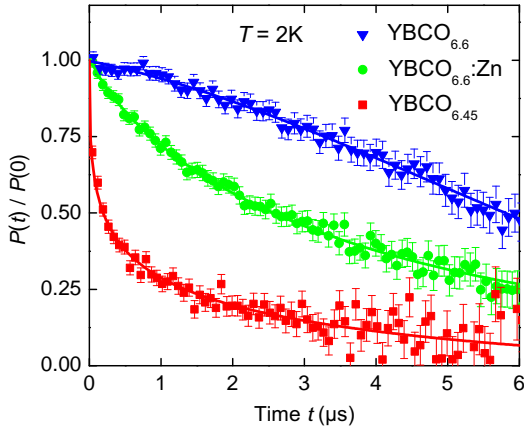


FIG. 2: (color online) Zero-field muon-spin relaxation data for $\text{YBCO}_{6.6}:\text{Zn}$ and reference samples $\text{YBa}_2\text{Cu}_3\text{O}_{6.6}$ and $\text{YBa}_2\text{Cu}_3\text{O}_{6.45}$ at $T = 2$ K. The lines are the results of fits described in the text.

quasielastic neutron signal like the one previously observed in $\text{YBCO}_{6.35}$ (Ref. 27) and $\text{YBCO}_{6.45}$ (Ref. 21) could not be detected above background [28], we performed muon spin relaxation (μSR) measurements, which are well suited to search for weak magnetic order. The experiments were performed with the GPS setup at the $\pi\text{m}3$ beamline at the Swiss muon source $S\mu\text{S}$ at the Paul Scherrer Institute, Villigen, Switzerland. The time-resolved μSR spectra of $\text{YBCO}_{6.6}:\text{Zn}$ as well as reference spectra of Zn-free $\text{YBCO}_{6.6}$ and $\text{YBCO}_{6.45}$ (Fig. 2) were fitted to the relaxation function $P(t) = P(0)\exp[(-\lambda t)^\beta] \times KT$ that consists of the product of a stretched exponential and a Kubo-Toyabe (KT) function, which account for the contribution of the electronic and nuclear magnetic moments, respectively. For $\text{YBCO}_{6.6}$ the relaxation is dominated by the nuclear moments, suggesting the absence of static or slowly fluctuating electronic moments. The $\text{YBCO}_{6.6}:\text{Zn}$ spectra exhibit a more rapid depolarization at temperatures below ~ 10 K (Fig. 2), which is a signature of dominant contributions from electronic moments. The absence of a precession frequency indicates that these electronic moments are either static and disordered or slowly fluctuating. The obtained values of $\beta \sim 0.4$ for $\text{YBCO}_{6.45}$ and $\beta \sim 0.7$ for $\text{YBCO}_{6.6}:\text{Zn}$ are characteristic of a spatially nonuniform distribution of the magnetic moment amplitude or fluctuation rate [16]. These observations confirm prior μSR results [1, 29, 30] according to which spinless impurities extend the range of magnetic order in the phase diagram of YBCO_{6+x} up to $x \sim 0.7$. The low-energy INS data (Fig. 1) and the close similarity between the μSR spectra of $\text{YBCO}_{6.6}:\text{Zn}$ and those of pure $\text{YBCO}_{6.45}$ (Fig. 2) now indicate that this order is incommensurate, in contrast to the commensurate antiferromagnetism suspected on the basis of prior INS data on $\text{YBCO}_{6+x}:\text{Zn}$ [12, 13].

We now describe the behavior of the spin system at higher temperatures and excitation energies. At $T = 70$ K (that is, above T_c of both $\text{YBCO}_{6.6}$ and $\text{YBCO}_{6.6}:\text{Zn}$), low-energy IC

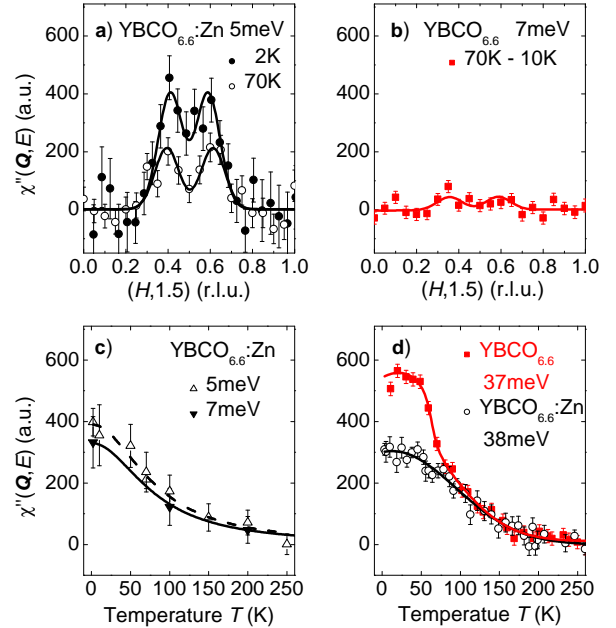


FIG. 3: (color online) Temperature dependence of the spin fluctuation intensity. (a,b) Scans of the dynamical magnetic susceptibility, $\chi''(\mathbf{Q}, E)$ (derived from the INS data by correcting for the detailed-balance factor), around $\mathbf{Q} = (0.5, 0.5, 1.7)$ in Zn-substituted and Zn-free $\text{YBCO}_{6.6}$ at energies and temperatures marked in the legend. The data were background-corrected as described in Fig. 1. The lines are the results of fits described in the text. (c) Amplitude of χ'' in $\text{YBCO}_{6.6}:\text{Zn}$ at $E = 5$ and 7 meV extracted from fits to constant-energy scans. (d) Amplitude of χ'' for $\text{YBCO}_{6.6}:\text{Zn}$ ($\text{YBCO}_{6.6}$) at $E = 38$ (37) meV. The lines are guides-to-the-eye.

fluctuations persist in $\text{YBCO}_{6.6}:\text{Zn}$ without significant thermal broadening (Fig. 3a), and remain much more intense than those in $\text{YBCO}_{6.6}$ (Fig. 3b). The onset temperature of the IC intensity in $\text{YBCO}_{6.6}:\text{Zn}$ is ~ 150 K (Fig. 3c), comparable to the onset of the spin-pseudogap in $\text{YBCO}_{6.6}$ previously documented by NMR [1]. This shows that Zn substitution restores low-energy spin fluctuations not only in the superconducting state, but also in the pseudogap state. The characteristic temperature for the Zn-induced enhancement of the spin dynamics is also comparable to the onset temperature of IC spin fluctuations in $\text{YBCO}_{6.45}$, which provides evidence for an electronic nematic state [20].

A converse spectral-weight shift is observed at higher energies. Pure $\text{YBCO}_{6.6}$ exhibits a sharp resonant mode with energy $E_{res} = 38$ meV in the superconducting state [22, 23], which is manifested by a sharp enhancement of the spin fluctuation intensity for $E \sim E_{res}$ below T_c (Fig. 3d). While $\text{YBCO}_{6.6}:\text{Zn}$ exhibits a similar narrowing of the magnetic response around Q_{AF} and $E = 38$ meV as pure $\text{YBCO}_{6.6}$ (Fig. 1f), followed by a dispersion away from Q_{AF} at higher energies (not shown), the superconductivity-induced anomaly is obliterated by Zn substitution (Fig. 3d). This is consistent with previous INS studies close to optimal doping that had demonstrated progressive weakening of the resonant mode

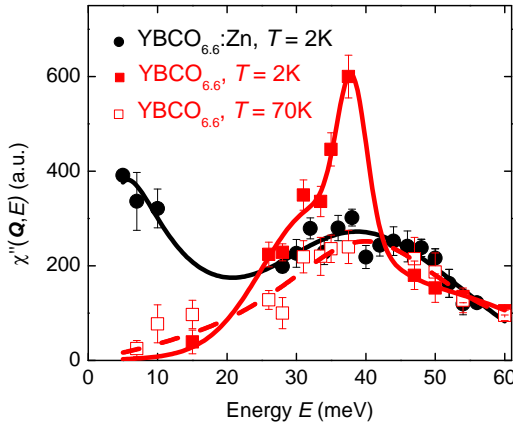


FIG. 4: (color online) Energy dependence of the peak susceptibility χ'' at $T = 2$ K extracted from constant-energy scans on $\text{YBCO}_{6.6}:\text{Zn}$ and $\text{YBCO}_{6.6}$. Normal-state data on pure $\text{YBCO}_{6.6}$ are shown for comparison. The lines are guides-to-the-eye.

with increasing Zn content without significant renormalization of its characteristic energy [31–33].

Figure 4 provides a synopsis of the spin excitation spectra of $\text{YBCO}_{6.6}$ and $\text{YBCO}_{6.6}:\text{Zn}$. The $\text{YBCO}_{6.6}:\text{Zn}$ spectrum at low temperatures is closely similar to the normal-state spectrum of $\text{YBCO}_{6.6}$, except for the strongly enhanced intensity at low energies that goes along with the appearance of IC magnetic order. The low-temperature spectrum of $\text{YBCO}_{6.6}$, on the other hand, is dominated by the sharp magnetic resonant mode at 38 meV, which is a signature of the superconducting state [23]. Fingerprints of both forms of collective electronic order are thus clearly apparent in the spin excitation spectrum, and the spectral-weight redistribution induced by Zn substitution demonstrates that spinless impurities nucleate static IC magnetism at the expense of superconductivity. This conclusion is consistent with the behavior expected in the vicinity of a quantum critical point separating both phases, and with prior μ SR studies that had indicated a local suppression of the superfluid density around Zn impurities [34, 35]. The two-phase competition also explains the extreme sensitivity of the magnetic resonant mode to a minute concentration of Zn impurities [31–33], which is difficult to explain in the framework of the random-phase approximation commonly used to describe the origin of this mode [36].

In conclusion, our experiments on the prototypical spin-pseudogap material $\text{YBCO}_{6.6}$ have shown that spinless impurities induce incommensurate magnetic order and low-energy spin excitations with a correlation range comparable to the mean distance between the impurities. In conjunction with prior data on LSCO [14, 15], this indicates a universal order-from-disorder phenomenology for copper oxides with 2D electronic structure, closely analogous to the one previously established for quasi-1D quantum magnets [2–4]. In contrast to the latter systems, however, the spin excitations in the layered copper oxides are incommensurate. Our demonstration that the incommensurability in the

YBCO_{6+x} system is independent of impurity concentration and controlled by the density of itinerant charge carriers, as previously shown for LSCO [14, 15, 18, 19], explains the difference to the Mott-insulating 1D systems and further underscores the universality of impurity-induced spin correlations in low-dimensional quantum magnets.

We acknowledge discussions with E. Fradkin, P.J. Hirschfeld, H.Y. Kee, S.A. Kivelson, and O.P. Sushkov, and financial support by the DFG under grant FOR538.

* Electronic address: b.keimer@fkf.mpg.de

† Electronic address: yvan.sidis@cea.fr

- [1] For a review, see H. Alloul *et al.* Rev. Mod. Phys. **81**, 45 (2009).
- [2] M. Hase *et al.*, Phys. Rev. Lett. **71**, 4059 (1993).
- [3] M. Azuma *et al.*, Phys. Rev. B **55**, R8658 (1997).
- [4] J. Bobroff *et al.*, Phys. Rev. Lett. **103**, 047201 (2009).
- [5] S. Sachdev *et al.*, Science **286**, 2479 (1999).
- [6] K.H. Höglund *et al.*, Phys. Rev. Lett. **98**, 087203 (2007).
- [7] M.A. Metlitski *et al.*, Phys. Rev. B **76**, 064423 (2007).
- [8] R.L. Doretto *et al.*, Phys. Rev. B **80**, 024411 (2009).
- [9] S. Wessel *et al.*, Phys. Rev. Lett. **86**, 1086 (2001).
- [10] M. Schmid *et al.*, arXiv:0912.2941.
- [11] J. Bobroff *et al.*, Phys. Rev. Lett. **89**, 157002 (2002).
- [12] Y. Sidis *et al.*, Phys. Rev. B **53**, 6811 (1996).
- [13] K. Kakurai *et al.*, Phys. Rev. B **48**, 3485 (1993).
- [14] H. Kimura *et al.*, Phys. Rev. Lett. **91**, 067002 (2003).
- [15] M. Kofu *et al.*, Phys. Rev. B **72**, 064502 (2005).
- [16] C. Panagopoulos *et al.*, Phys. Rev. B **69**, 144510 (2004).
- [17] S.A. Kivelson *et al.*, Rev. Mod. Phys. **75**, 1201 (2003).
- [18] H. Kimura *et al.*, Phys. Rev. B **59**, 6517 (1999).
- [19] M. Kofu *et al.*, Phys. Rev. Lett. **102**, 047001 (2009).
- [20] V. Hinkov *et al.*, Science **319**, 597 (2008).
- [21] D. Haug *et al.*, Phys. Rev. Lett. **103**, 017001 (2009).
- [22] V. Hinkov *et al.*, Nature Phys. **3**, 780 (2007).
- [23] H.F. Fong *et al.*, Phys. Rev. B **61**, 14773 (2000).
- [24] I.G. Kaplan *et al.*, Phys. Rev. B **65**, 214509 (2002).
- [25] A.A. Abrikosov, Physica C **397**, 77 (2003).
- [26] S. Ouazi *et al.*, Phys. Rev. B **70**, 104515 (2004). Note that the “impurity correlation length” ξ_{imp} defined in this paper is a factor of two larger than the length ξ extracted from the momentum half-width of the neutron profiles.
- [27] C. Stock *et al.*, Phys. Rev. B **73**, 100504(R) (2006).
- [28] Note that the intensity of the quasielastic neutron signal reported for $\text{YBCO}_{6.45}$ [20, 21] is at the edge of the detection limit. Since the volume of the present $\text{YBCO}_{6.6}:\text{Zn}$ sample is factor of three smaller, and the ordered moment is weaker (Fig. 3), the quasielastic signal is expected to be below the detection limit, in agreement with the data.
- [29] P. Mendels *et al.*, Phys. Rev. B **49**, R10035 (1994).
- [30] C. Bernhard *et al.*, Phys. Rev. B **58**, R8937 (1998).
- [31] H.F. Fong *et al.*, Phys. Rev. Lett. **82**, 1939 (1999).
- [32] Y. Sidis *et al.*, Phys. Rev. Lett. **84**, 5900 (2000).
- [33] Y. Sidis *et al.* in *Open Problems in Strongly Correlated Electron Systems* (Kluwer, 2001); arXiv:0006265.
- [34] C. Bernhard *et al.*, Phys. Rev. Lett. **77**, 2304 (1996).
- [35] B. Nachumi *et al.*, Phys. Rev. Lett. **77**, 5421 (1996).
- [36] N. Bulut, Phys. Rev. B **61**, 9051 (2000).